

Zeitschrift: IABSE congress report = Rapport du congrès AIPC = IVBH
Kongressbericht

Band: 8 (1968)

Artikel: Prestressed reinforced concrete system

Autor: Yokomichi, Hideo

DOI: <https://doi.org/10.5169/seals-8838>

Nutzungsbedingungen

Die ETH-Bibliothek ist die Anbieterin der digitalisierten Zeitschriften auf E-Periodica. Sie besitzt keine Urheberrechte an den Zeitschriften und ist nicht verantwortlich für deren Inhalte. Die Rechte liegen in der Regel bei den Herausgebern beziehungsweise den externen Rechteinhabern. Das Veröffentlichen von Bildern in Print- und Online-Publikationen sowie auf Social Media-Kanälen oder Webseiten ist nur mit vorheriger Genehmigung der Rechteinhaber erlaubt. [Mehr erfahren](#)

Conditions d'utilisation

L'ETH Library est le fournisseur des revues numérisées. Elle ne détient aucun droit d'auteur sur les revues et n'est pas responsable de leur contenu. En règle générale, les droits sont détenus par les éditeurs ou les détenteurs de droits externes. La reproduction d'images dans des publications imprimées ou en ligne ainsi que sur des canaux de médias sociaux ou des sites web n'est autorisée qu'avec l'accord préalable des détenteurs des droits. [En savoir plus](#)

Terms of use

The ETH Library is the provider of the digitised journals. It does not own any copyrights to the journals and is not responsible for their content. The rights usually lie with the publishers or the external rights holders. Publishing images in print and online publications, as well as on social media channels or websites, is only permitted with the prior consent of the rights holders. [Find out more](#)

Download PDF: 13.01.2026

ETH-Bibliothek Zürich, E-Periodica, <https://www.e-periodica.ch>

Prestressed Reinforced Concrete System

Le système du béton armé précontraint

Stahlbeton mit Spannzulagen (Vorgespannter Stahlbeton)

HIDEO YOKOMICHI

Dr. Eng., Professor, Faculty of Engineering
Hokkaido University, Sapporo, Japan

1. Introduction

The "Prestressed Reinforced Concrete (PRC)" system is defined as a system in which relatively small prestressing forces are introduced into reinforced concrete (RC) in attempt to reduce the opening of cracks. In this case, the RC is designed to have the required safety factor against failure. The conditions to be met for tolerable crack opening in PRC is the same as in RC. In other words PRC is a partially prestressed concrete with mixed reinforcement.

The term "Prestressed Reinforced Concrete (PRC)" was proposed by the author's team in 1961, to distinguish PRC from the full or limited prestress system used hitherto. The main difference between the two systems is as follows; the basic system of PRC is reinforced concrete while that of the latter is plain concrete in the absence of prestressing forces.

The PRC system combines the merits of RC and prestressed concrete (PC) in that the cost is low as in RC and that the cracking behavior is advantageous as in PC. Allowing for tolerable crack openings of 0.1 to 0.3mm, the prestressing forces in this system are generally small not exceeding about one fifth of ordinary limited prestressed concrete.

The author's team have continued to study the PRC system since 1961 and have constructed several bridges, including a 48m span of π -shaped rigid frame.

In this paper the behavior of PRC beams in cracking and deformation are discussed on the basis of the results of tests on a total of 250 RC tensile elements and a total of 200 RC beams and PRC beams under static and dynamic loads with less than 2 million pulsations. Design rules of PRC are derived for controlling crack width.

The present paper also describes the practical aspects of PRC and the Kamihimekawa bridge designed according to the system.

2. Cracking and Deformation

2.1 Introduction

For rational designing of RC and PRC structures, it is necessa-

try to clarify beforehand the behavior of cracking and deformation. Many investigations on this problem have been carried out in many countries, for recent instances (1)(2)(3). In the present paper results on the analysis of tension elements and of beams that were obtained in the investigations (4 to 9) are applied. Efforts are made to render the design rules as simple as possible without losing theoretical scrutinization throughout the course.

Particular stress is laid on the hyperbolic-cosine behavior in the initial state of cracking and the effect of the concrete cover in the stationary state.

2.2 Maximum Crack Spacing and Maximum Crack Width

2.21 Fundamental Equations

Distances between cracks observed in RC tension elements and beams generally vary over a wide range between maximum and minimum values. However, the maximum crack spacing is to be theoretically estimated (4).

Let tensile force P be gradually increased in a tension test of a bar surrounded by concrete of a length, l , as shown in Fig.1, and a crack be first observed in the mid section at $P = \sigma_{so} A_s$, then the length, l , is to be considered as equal to the maximum crack spacing at P , denoted by l_{max}^P . Thus, applying the equilibrium equation

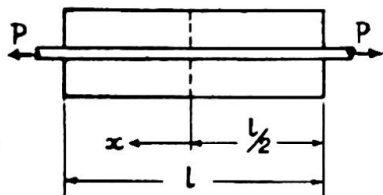


Fig.1

$$l_{max}^P = \frac{2 k_1 A_e \sigma_{ct}}{U \bar{\tau}_o^P} \quad (1)$$

where

A_e = cross-sectional area of concrete of the element,
 σ_{ct} = tensile strength of concrete,
 $\bar{\tau}_o$ = mean value of bond stresses over the length, l ,
 U = perimeter of steel bar,
 k_1 = coefficient.

Following the first cracking, new cracks occur in succession under progressively increasing loads. However, this phenomenon terminates at a critical value of the steel stress $\hat{\sigma}_{so}$, shown in Fig.2 (4), after which only an increase in crack width is seen. From the test results (4) $\hat{\sigma}_{so}$ in the case of deformed bars was found equal to 1.5 to 2.5 times $\sigma_{so,cr}$ which is the steel stress at the first cracking.

Thus the cracking behavior of RC tensile elements and beams may be divided into two different states; i.e. the initial state of cracking with steel stresses of $\sigma_{so} < \hat{\sigma}_{so}$ and the stationary state of cracking with $\sigma_{so} \geq \hat{\sigma}_{so}$. In practice it is necessary to clarify the behavior in the initial state of cracking, because this state often occurs under working loads.

The crack width, w , can generally be expressed by

$$w = \left(\frac{\sigma_{so}}{E_s} - \frac{\bar{\sigma}_{cm}}{p E_s} - \bar{\epsilon}_{c,surf} \right) l,$$

where l = crack spacing,

σ_{so} = steel stress in the cracked section,

$\bar{\sigma}_{cm}$ = mean concrete stress in a given section,

$\bar{\sigma}_{cm}$ = mean value of σ_{cm} over the length l ,

p = ratio of cross-sectional area of the bar A_s against that of concrete A_e ,

$\bar{\epsilon}_{c,surf}$ = mean strain at the surface of concrete over the length, l .

$\bar{\epsilon}_{c,surf}$ involves elastic strain, plastic residual strain, pre-

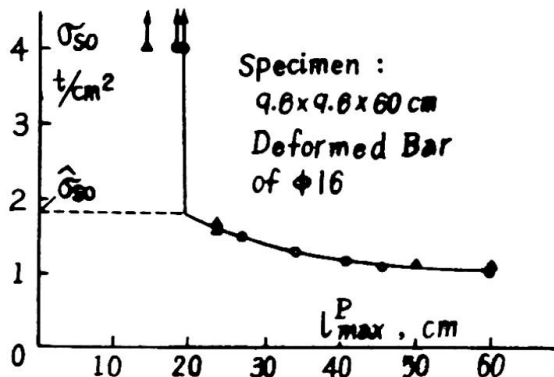


Fig. 2

strain etc. and is generally smaller than other strains, except where prestrain and shrinkage are important. In practice it may be disregarded. Thus, the crack width can be expressed by

$$w = \left(\frac{\sigma_{so}}{E_s} - \frac{\bar{\sigma}_{cm}}{p E_s} \right) l \quad (2)$$

$\bar{\sigma}_{cm}$ depends on the steel ratio, p , and the tensile strength of concrete, σ_{ct} . Investigation (4) shows that the relation between $\bar{\sigma}_{cm}/\sigma_{ct}$ and p , (Fig. 3) is available for utilization in the case of deformed bars, irregardless of the change in diameter of the bars.

Further, from eq.(2), the steel stress, $\sigma_{so,w}$, at which the crack width at spacing l reaches a certain value of w can be expressed by

$$\sigma_{so,w} = \frac{E_s w}{l} + \frac{\bar{\sigma}_{cm}}{p}. \quad (3)$$

2.22 Initial State of Cracking

Let the straight line 1-2-1 shown in Fig.4 be the original sectional plane in RC tensile element of the abscissa of x indicated in Fig.4 and let the curved line 1'-2'-1' be its actual deformed surface and let the line 1"-2"-1" be the mean level of the sectional surface of concrete, then, with regard to the difference between the elongation of steel bar A_s and the mean deformation A_{cr} , the following differential equation is obtained by assuming that the deformation of concrete in the section is caused only by shear stresses (4)

$$\frac{d^2A}{dx^2} - k_3^2 A = 0, \quad (4)$$

where $k_3^2 = \beta G_c \frac{U}{t} \left(\frac{1}{A_s E_s} + \frac{1}{A_e E_c} \right)$
 $\beta = \frac{\gamma_i}{\gamma_m \beta_1}$

Solving the differential equation, A can be expressed by

$$A = \frac{\sigma_{so}}{k_3 E_s} \frac{\sinh k_3 x}{\cosh k_3 l/2} \quad (5)$$

accordingly the following expressions can be derived

$$\sigma_s(x) = \frac{\sigma_{so}}{1+np} \left(np + \frac{\cosh k_3 x}{\cosh k_3 l/2} \right), \quad (6)$$

$$\sigma_{cm}(x) = \frac{p \sigma_{so}}{1+np} \left(1 - \frac{\cosh k_3 x}{\cosh k_3 l/2} \right). \quad (7)$$

The tests (4) shows that the coefficient β in eq.(4) can be equal to 0.25. Taking into consideration the fact that

$$\sigma_{cm}(0) = \sigma_{ct} \quad \text{and} \quad P_{cr} = \sigma_{ct} A_i,$$

the maximum crack spacing in the initial state may be derived from eq.(7) by a hyperbolic-cosine function

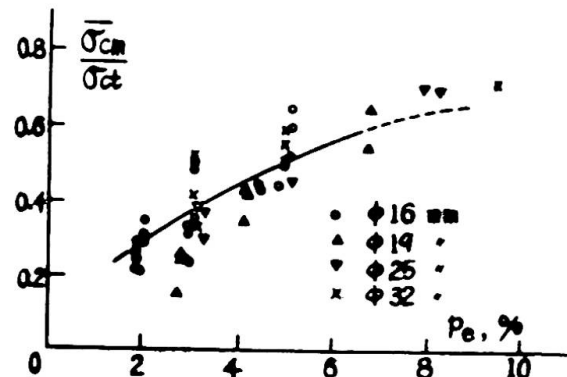


Fig. 3

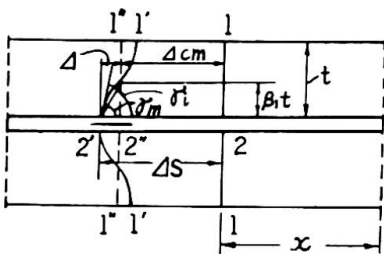


Fig.4

A number of flexural tests on rectangular and T-shaped RC beams with a span of 3.0m also shows that the theoretical line of l^P_{max} expressed by eq.(8) is in fairly good agreement with the limiting line of the scattered plotted points as indicated in Fig.5.

$$l^P_{max} = \frac{2}{k_3} \cosh^{-1} \frac{P}{P - P_{cr}}. \quad (8)$$

A number of tension tests of bars surrounded by concrete (4) shows that the theoretical line of l^P_{max} expressed by eq.(8) is in fairly good agreement with the limiting line of the scattered plotted points as indicated in Fig.5.

Fig.4
A number of flexural tests on rectangular and T-shaped RC beams with a span of 3.0m also shows that the theoretical line of l^P_{max} expressed by eq.(8) is in fairly good agreement with the limiting line of the scattered plotted points as indicated in Fig.5.

$$l^M_{max} = \frac{2}{k_3} \cosh^{-1} \frac{M}{M - M_{cr}} \quad (9)$$

and as A_e in eq.(4) an effective sectional area of concrete in which the center of gravity coincides with that of the reinforcing bar, Fig.7. Furthermore, taking into consideration that $4(x = l/2) = w/2$ and combining eq.s(5) and (9), maximum crack width can be expressed by

$$w^M_{max} = \frac{2}{k_3} \frac{\sigma_{so}}{E_s} \frac{\sqrt{M_{cr}(2M - M_{cr})}}{M}. \quad (10)$$

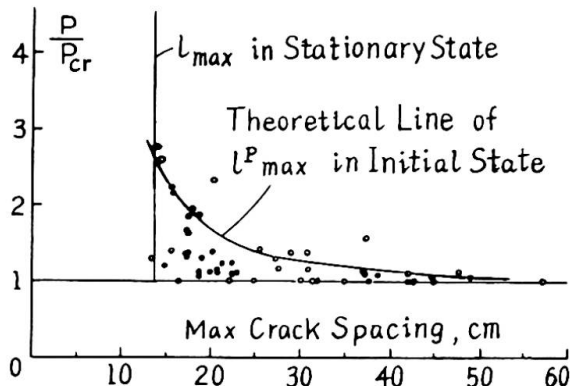


Fig.5

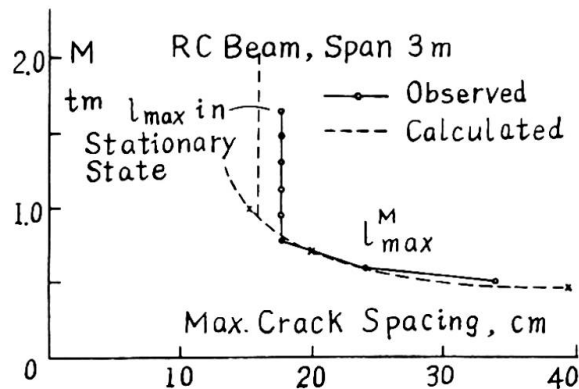


Fig.6

2.23 Stationary State of Cracking

In this state the number of cracks no longer increases; hence maximum crack spacing is constant. The maximum crack spacing in this state is denoted by l_{max} and the following expression is obtained from eq.(1)

$$l_{max} = \frac{2 k_1 A_e \sigma_{ct}}{U(\bar{\tau}_o)_{max}}. \quad (11)$$

Since $U\bar{\tau}_o$ expresses the force per unit length, transmitted by bond to the surrounding concrete, its maximum value is affected by the values of σ_{ct} , A_e , concrete cover, t , and also by the pattern of bars. Investigation (4)

shows that $U(\bar{\tau}_o)_{max}/\sigma_{ct}$ is fairly proportional to A_e/t_{mean} as shown in Fig.8. Taking this into consideration, a simple expression can be obtained from eq.(10)

$$l_{max} = k_2 t_{mean} \quad (12)$$

where t_{mean} denotes the mean of concrete covers, $(t_1 + t_2)/2$, in case of the sections as indicated in Fig.7. Applying eq.(2), the maximum crack width in the stationary state is expressed by

$$w_{max} = \left(\frac{\sigma_{so}}{E_s} - \frac{\sigma_{cm}}{p E_s} \right) l_{max}. \quad (13)$$

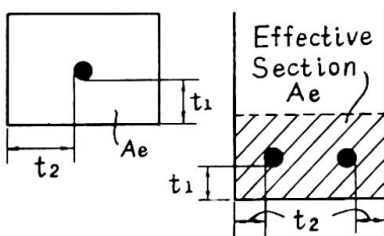


Fig.7

Fig.7
In this state the number of cracks no longer increases; hence maximum crack spacing is constant. The maximum crack spacing in this state is denoted by l_{max} and the following expression is obtained from eq.(1)

$$l_{max} = k_2 t_{mean} \quad (12)$$

where t_{mean} denotes the mean of concrete covers, $(t_1 + t_2)/2$, in case of the sections as indicated in Fig.7. Applying eq.(2), the maximum crack width in the stationary state is expressed by

$$w_{max} = \left(\frac{\sigma_{so}}{E_s} - \frac{\sigma_{cm}}{p E_s} \right) l_{max}. \quad (13)$$

Tests (4) on a total of 250 of RC tensile elements show that the coefficient k_2 in case of deformed bars with transverse ribs is 5.4 (Fig.9). A number of tests on RC beams with a span of 3.0m show that eq.(13) and eq.(12) are valid (Fig.10)(4).

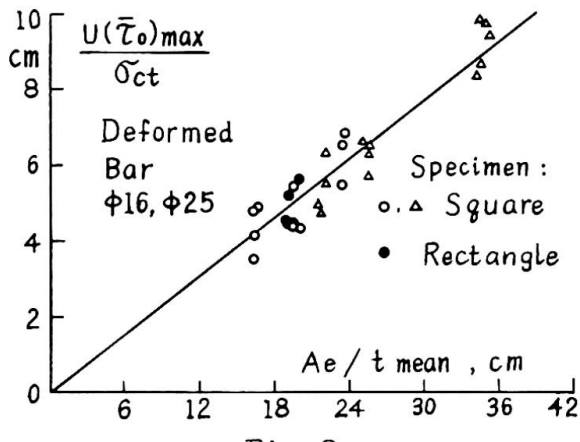


Fig.8

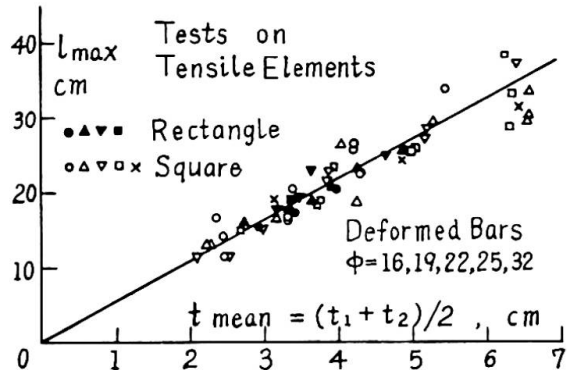


Fig.9

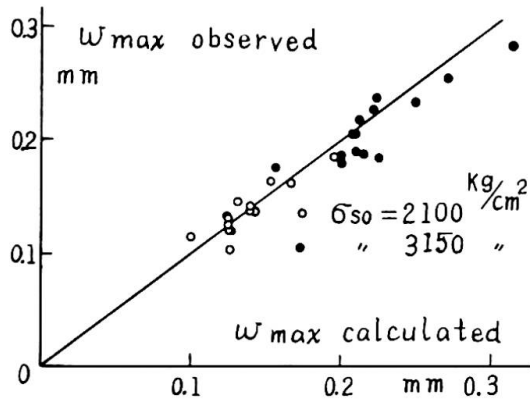


Fig.10

iting lines within a range of $\pm 2 \times$ standard deviation are in the figure.

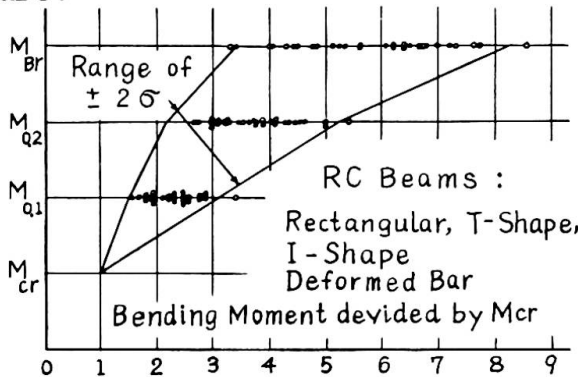


Fig.11

Thus, the following approximate expressions can be adopted for practical use

$$M_{0.1} \geq 1.4 M_{cr} \quad \text{and} \quad M_{0.2} \geq 2.0 M_{cr} \quad (14)$$

With reference to the estimation of cracking moment M_{cr} , existing materials will serve well (7)(10).

Secondly a more precise determination of the moment M_w for maximum crack width of w in state II is expressed by

$$M_w = \sigma_{so,w} A_s z, \quad (15)$$

where z = lever arm of resisting couple in the cracked section. $\sigma_{so,w}$ is obtained by combining eq.s(3), (12) and (13). A chart for $\sigma_{so,w}$ -

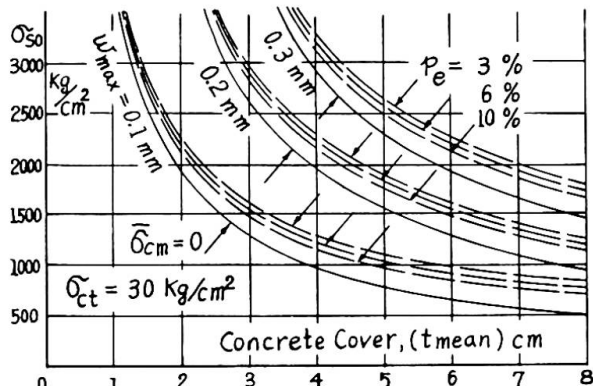


Fig.12

Concrete Cover, (t mean) cm

relations are indicated in Fig.12, showing the effects of variations of κ . In state I, where w_{max} is approximately less than 0.1mm, directly from eq.(10) M_w is expressed by

$$M_w = \frac{1}{2} M_{cr} + (w \kappa_3 E_s A_s z)^2 / 8 M_{cr} \quad (16)$$

2.3 Cracking Behavior of PRC Beams

Tests (4)(5) were performed for comparing the cracking behavior of PRC beams against that of RC beams. T-section or rectangular sections of 30cm height and a 3m span were used. As regards the crack width steel strain diagrams showed little or no difference between the two systems (Fig.13). Σw in the figure gives the sum of crack widths observed in the middle third of the span where bending moments are constant and ε_{so} is the steel strain in the cracked section. Moreover, the results show a characteristic behavior of PRC beams in moment-crack width relation (Fig.14).

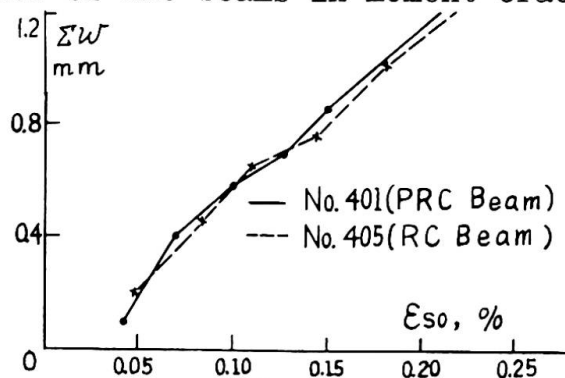


Fig.13

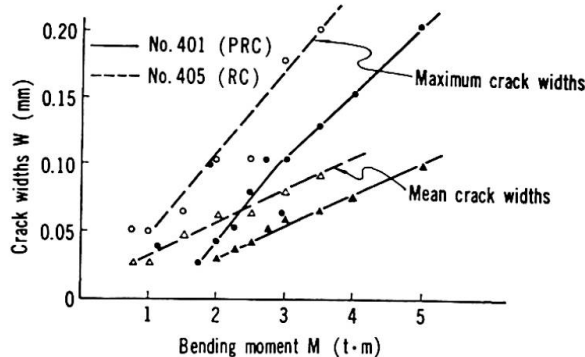


Fig.14

By the action of prestressing forces P_v the cracking moment leading to the first cracks increases approximately by the amount

$$\Delta M = P_v (e_p + \kappa') \quad (17)$$

where e_p and κ' are the distances from the gravity center to the position of prestressing tendons and to the core point for the tension edge, respectively. In the cracked state the effect of prestress on the reduction of crack widths is strengthened with the development of cracks, i.e. with the increase of load (Fig.14). This shows that PRC is practical, because in PRC beams the prestress aims at the restraint of the development of crack widths, namely, the reduction of stress of the reinforcement under dead load in the cracked state, while in the PC system the prestress aims at complete prevention of cracks and is much greater in magnitude than the former.

Thus the following expression for the increment in M_w in eq.(15) by P_v can be obtained from Fig.14

$$\Delta M = P_v (z - \Delta e) \quad (18)$$

where Δe = distance from RC steel to PC tendon

2.4 Deformation in Cracked State

In the uncracked state the moment-deflection line of RC beams is approximately linear as shown in Fig.15, its direction I being calculated by an ordinary hypothesis of "State I" in which a complete section of concrete is considered. Following the first cracking under increasing loads, the line suddenly changes its direction and turns gradually to have an approximately constant direction II₀ nearly parallel to the straight line II. The inclination is determined by the usual hypothesis of the "State II" where the tensile strength is disregarded and Bernoulli's assumption and Hooke's law are valid.

Though the transition line between the two straight lines, I

and II_0 , is generally pretty complicated, for practical use it can approximately be substituted by a straight line III as indicated in the figure, which intersects the lines I and II_0 at points A and B respectively. The two points can be assumed to correspond to the previously mentioned steel stresses $\bar{\sigma}_{so,cr}$ and $\bar{\sigma}_{so}$ respectively.

Moreover, since the vertical distance, ΔM , between the two lines II_0 and II is considered to be caused by the effectiveness of the tensile strength of concrete in the tensile zone between cracks, the moment-deflection line II_0 can theoretically be calculated (4) or approximately be expressed by

$$M(\delta) = M_{II}(\delta) + \Delta M, \quad \Delta M = (A_e + 0.3A_{ew})\bar{\sigma}_{cm}y_e = \text{constant} \quad \{ \quad (19)$$

where A_e = effective sectional area of concrete in tension zone, Fig.7,

A_{ew} = sectional area of a part of the web obtained by subtracting A_e from the total sectional area of concrete in the tension zone,

y_e = distance from gravity-center of complete section of concrete to that of effective section.

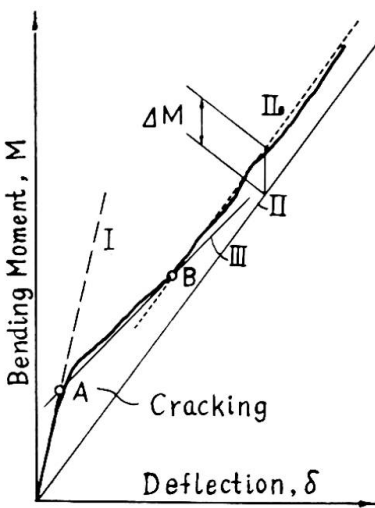


Fig.15

For values of $\bar{\sigma}_{cm}$ Fig.3 is available as previously mentioned.

3. Influences of Delayed Deformation and Fatigue on Cracking and Deformation Behavior of Beams

3.1 Delayed Deformation

The deflection of a beam due to creep of concrete under a sustained load, is partially restricted by reinforcing steels. However the eccentric restriction of concrete shrinkage by steel exerts a fairly large supplemental deflection of a beam. The restriction effect of both reinforcing bars and PC tendons in PRC beams can theoretically be analyzed (4)(5), but in most cases of PRC beams the restriction by PC tendons is negligible. Tests mentioned previously (4)(5) show the validity of the above-stated behavior as shown in Fig.16.

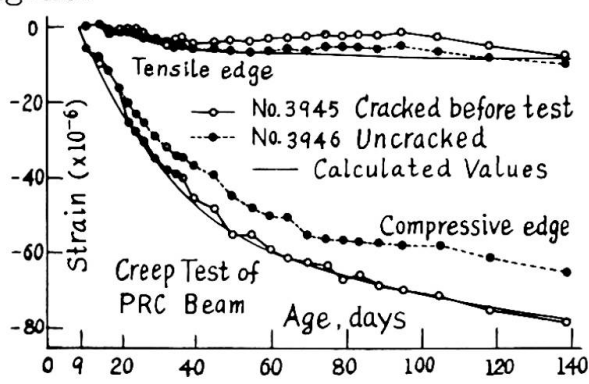


Fig.16

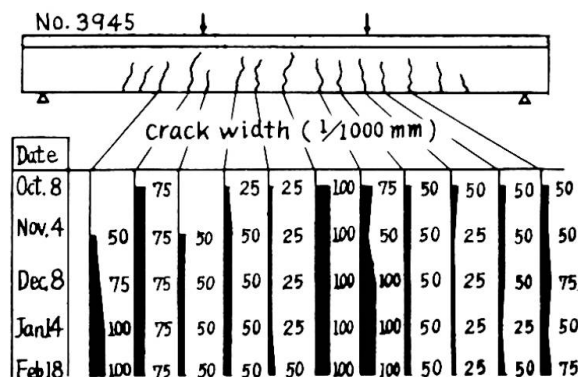


Fig.17

The crack widths observed in PRC beams remain practically unchanged under sustained load (Fig.17)(4)(5). A precise investigation on RC beams (4) shows that the increase of crack widths due to gradual relaxation of bond stresses are observed under sustained load, (Fig.18). The final amount of increment can theoretically be estimated as equal to $\bar{\sigma}_{cm}/p\bar{\sigma}_{so}$ in ratio against the initial crack

widths. As seen in Fig.18, however, this relaxation does not necessarily result in a detrimental failure of the bonds, because the static flexural test after creep test shows that the bond stresses are restored at higher loads than that in the creep test.

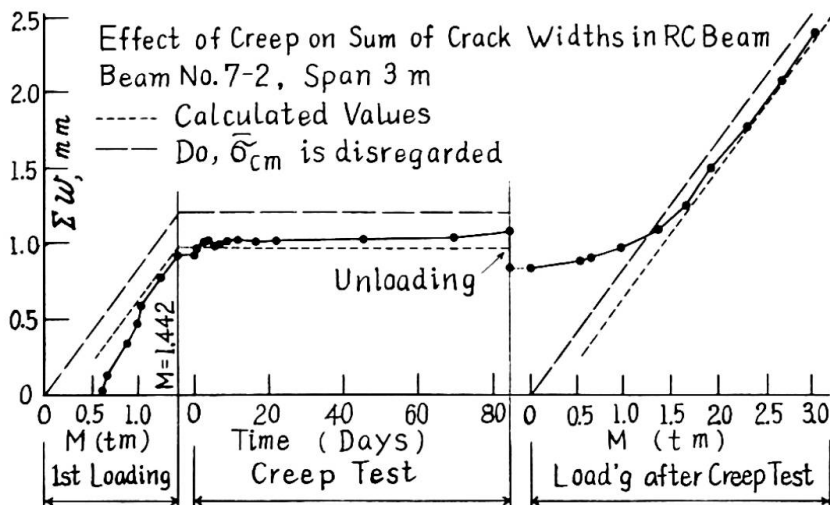


Fig.18

at a rate of 250 cycles per minute (4)(8)(9). The results show that the increase of crack openings and deflections hardly occurs by dynamic loads, when steel stresses σ_{s0} are under $0.8 \sigma_{sy}$, even when the initial crack openings were 0.3mm. Fig.19 shows a typical PRC test result.

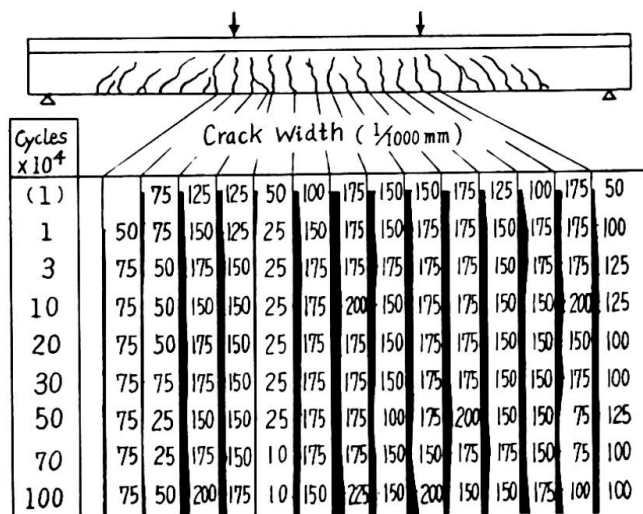


Fig.19

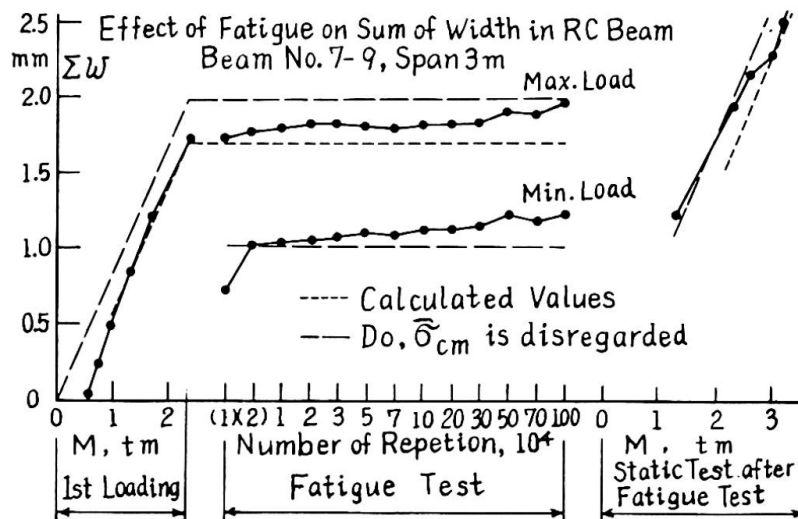


Fig.20

About 100 RC and PRC beams with T-shape cross sections of 28 x 30cm and reinforcing deformed bars were tested under repeated loads with less than two million pulsations

3.2 Fatigue

dynamic loads, when steel stresses σ_{s0} are under $0.8 \sigma_{sy}$, even when the initial crack openings were 0.3mm. Fig.19 shows a typical PRC test result.

A more precise investigation on RC beams (4) shows that a slight increase of crack widths is observed under repeated loadings (Fig.20), but this may be caused by gradual relaxation of bond stresses, as in creep tests previously mentioned.

4. Practice of PRC

As discussed the behavior of PRC in cracking and deformation, as influenced by creep and fatigue of concrete, is generally the same or increasingly advantageous than in RC. Accordingly in designing PRC the same safety conditions for tolerable opening of cracks in RC is sufficient. The safety conditions of cracking are generally specified as follows:

$$\text{Dead load } M_{w1} \geq f_1 M_D \quad (20)$$

$$\text{Live load } M_{w2} \geq f_2 M_L + M_D \quad (21)$$

where w_1 and w_2 are specified tolerable crack openings.

In the PRC system structures are firstly designed by RC theory to secure the required safety factor against failure. Then the bending moment M_w of each section is estimated, where M_w is the moment when maximum crack width in concrete reaches a specified value of w . M_w is determined by design rules as stated in 2.24.

Next, applying the calculated M_w the conditions (20)(21) are examined. When prestresses are required in certain sections, which generally occurs only with respect to condition (20), prestressing forces to be introduced using eq.s (17) and (18) are determined by

$$P_v \geq \frac{f_c M_p - M_{w1}}{Z - 4e}, \quad (22)$$

$$P_v \geq \frac{f_c M_p - M_{w1}}{e_p + k}, \text{ for } w_1 \leq 0.1 \text{ mm.} \quad (23)$$

Prestressing forces in this system determined as above are generally small not exceeding about one fifth of ordinary PC systems. Therefore concrete stresses which are superimposed by prestressing on the stresses due to working loads are generally very small and do not require checking. Thus the layout of prestressing tendons in a PRC system are easier than in PC systems.

Prestressing tendon arrangement is not always necessary for the full span of the structures. They may be arranged as outside or inside webs and also be designed by any system of pretensioning and posttensioning.

Before prestressing the elements of the structures designed for PRC system can withstand the loads during construction as RC elements. Hence prestressing can be done any time during construction. This fact is favorable, especially in the case of cantilever construction, and it is superior to ordinary PC systems in which pre-stresses must be introduced at every step of the construction.

5. Kamihimekawa Bridge

The Kamihimekawa bridge, over which national road No.5 runs is 40km north of Hakodate in southern Hokkaido, and is the first PRC (prestressed reinforced concrete) bridge constructed in Japan (11)

The main span is 48m, the two cantilever spans are 15.9m and the two piers are 19m high, forming a π -shaped rigid-frame structure of 80m. The carriageway is 7m wide and has a curved route with a radius of 400m, Fig.21.

A system of RC cantilevers was chosen for the construction of deck girders, which project from the piers. This was achieved by extending cantilevers by a RC system without prestressing or any centering.

The height of girders varies from 2.8m at the point, where it is rigidly fixed to the pier, to 1.2m at mid-span and to 2.0m at the end of cantilever span.

The transverse section of the structure consists of a 5m wide box-section. The upper slab of the box has a thickness of 22cm which is increased, by means of haunches, to 33cm at the junction with webs. The thickness of the lower slab varies from 15cm at mid-span to 50cm at the pier and 29cm at the point on the cantilever at 11.5m distance from the center of pier. The two webs of the girders have a constant thickness of 45cm.

The shaft of piers has a bi-cellular box-section, which is 2.0m \times 5.0m in outer measurements with a 40cm wall and is secured at the foundations.

Each half-span and cantilever girder were constructed by suc-

cessive corbellings, in a symmetrical manner, from the piers. The static calculations of the structure were performed for two states of structural systems, i.e. a system of cantilevers during construction and that of rigid frame after closing.

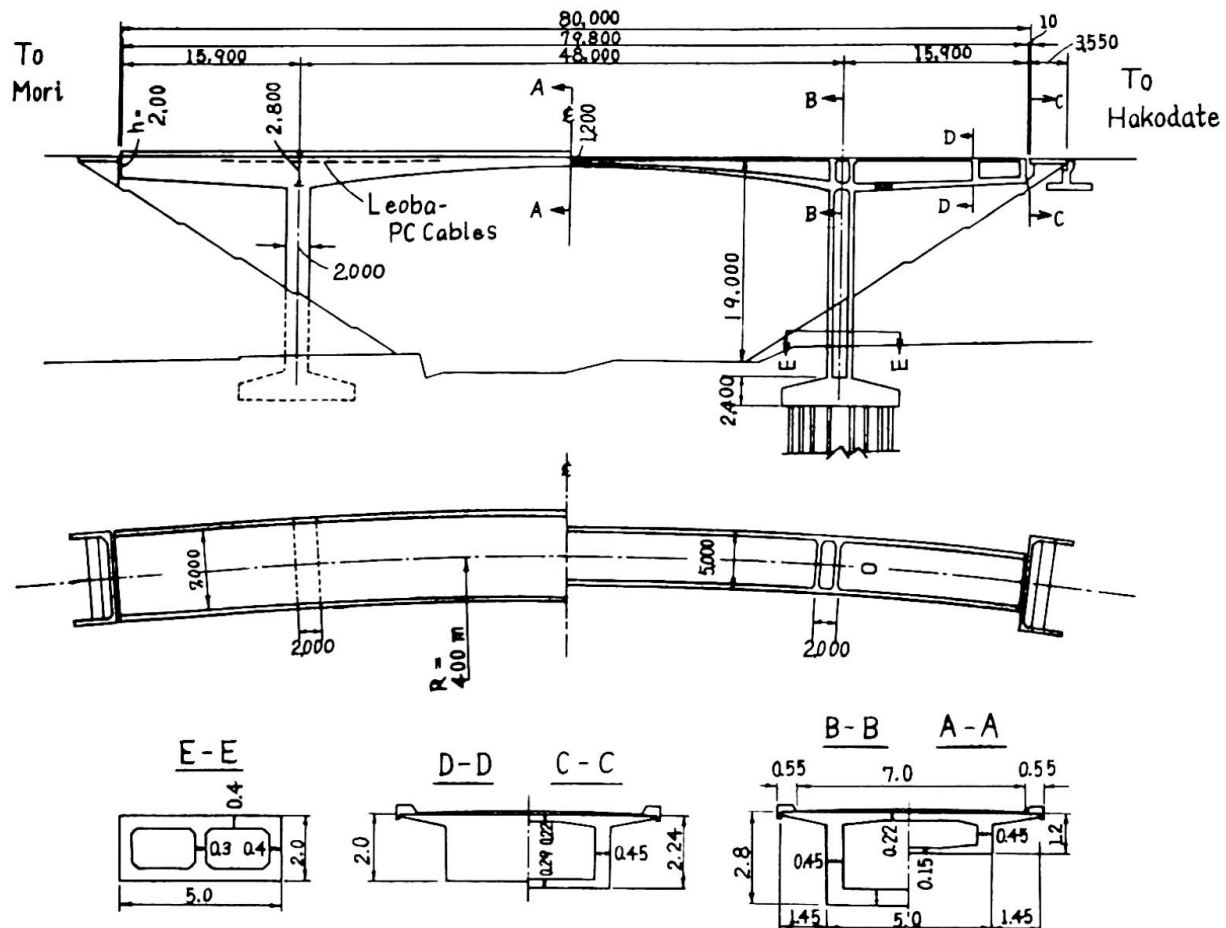


Fig.21 Kamihimekawa Bridge (Japan)

Before the closing 25.4t of ballasts were loaded temporarily on each end of the cantilever girders as a counter weight to balance the self weight of each girder of half length of center-span, Fig.



Fig.22
crete of $\sigma_{28} = 360 \text{ kg/cm}^2$ quality for piers.

A total of 470t of prestressing forces were longitudinally introduced during the corbelling construction to parts of deck girders of 22m length in order to control crack widths, Fig.21. The prestressing was performed in accordance with the Leoba system in two webs of

22.
The effect of delayed deformation of concrete as well as that of uplifts caused by removal of the counter weights after closing are to be taken into account for the static calculation.

The structure was designed as a RC system, using 32mm cold-twisted bars of steel SDC 40 as the main reinforcement and con-

crete of $\sigma_{28} = 210$ for the main girder and $\sigma_{28} = 360 \text{ kg/cm}^2$ for the piers.

the box girder by means of prestressing tendons which consist of the $6 \times S66(16\phi 8)$ and $2 \times S24(12\phi 5)$.

The super structure was built by corbelling in successive stages without centering. The length of the successive advances, which numbered 20 in all, was 3.0m. In accordance with the progress of the girders, the non-prestressed main bars $\phi 32$ were screwed to the next bars of 6m length by means of FY-couplers, Fig.23.

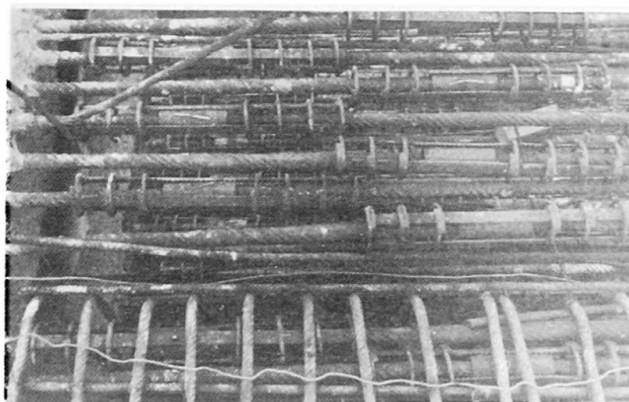


Fig.23

The FY-coupler is a special type of screw-threaded coupler which was developed by the author's team and experimentally tested to secure the transmission of the entire strength of the bar to be joined (12).

The main structure was completed in Nov. 1965 and the bridge was opened to traffic in June 1966. Fig.24 shows the completed bridge.



Fig.24 The completed Kamihimekawa Bridge

Acknowledgement

The author is grateful to Dr.Y.Kakuta for his assistance in the investigations and is also indebted to Dr.M.Hayashi, head of Division I of the Civil Engineering Research Institute of the Hokkaido Development Bureau, for his efforts in the development of the PRC system.

References (J: in Japanese)

1 Recommendations for an International Code of Practice for Rein-

forced Concrete-CEB, published by ACI,CCA,1963.

- 2 B.B.Broms:Cracking width and Crack Spacing in Reinforced Concrete Members,ACI-Journal, Vol.62, No.10, Oct.1965.
- 3 J.F.Borges:Cracking and Deformability of Reinforced Concrete Beams, IABSE-Publications 26th Volume,1966.
- 4 Y.Kakuta:Fundamental Investigation on Cracking and Deformation Behavior of Reinforced Concrete Beams,(J),Dissertation,Yokomichi Laboratory, Faculty of Eng., Hokkaido University, Dec.1967.
- 5 H.Yokomichi,Y.Kakuta:On Influence of Creep and Shrinkage of Concrete on Strain of PRC Beams,(J),Cement Gijitsu Nempo XX 1966, JCEA.
- 6 H.Yokomichi,Y.Fujita:Flexural Tests on Reinforced Concrete Beams with Deformed Bars,(J),Concrete Libraly No.2, Japan Society of Civil Engineers,1962.
- 7 Y.Fujita:Study on Ultimate Strength Design of Reinforced Concrete Beams and Prestressed Concrete Beams subjected to Simple Bending, (J), Bulletin of Faculty of Eng.,Hokkaido University No.32,Oct.1963
- 8 H.Yokomichi:On New Development of Reinforced Concrete and PRC System,(J),Hokkaido Branch of Japan Society of Civil Engineers, Feb.1964.
- 9 H.Yokomichi,Y.Fujita,T.Nishibori:On Fatigue Behavior of Concrete Beams Reinforced by Deformed Bars,(J),Reports of Civil Engineering Research Institute,Hokkaido Development Bureau,No.37, Oct.1965.
- 10 H.Yokomichi:Concrete Bridges,(J),Gihodo Co.Ltd., Tokyo,1962.
- 11 H.Yokomichi,S.Tonozaki:On Design and Execution of Kamihimekawa-bridge(PRC System),(J),Journal of Japan Prestressed Concrete Association Vol.7 No.5, Oct.1965.
- 12 Tests on FY-Coupler Joints of Deformed Bars,(J),Yokomichi Laboratory, Faculty of Eng., Hokkaido University, May 1965.

SUMMARY

The behavior of "prestressed reinforced concrete(PRC)" in cracking and deformation under static and dynamic loads is discussed. With regard to the cracking behavior the initial and stationary states are dealt with. The design rules for controlling the crack widths are derived. This paper also described the practical aspects of the PRC System and its application in the construction of the Kamihimekawa bridge, a π -shaped rigid frame bridge.

RÉSUMÉ

Les agissements du béton armé précontraint dans la fissuration et la déformation sous les charges statiques et dynamiques sont discutés. Concernant des agissements de la fissuration, les conditions initiales et stationnaires sont traitées. Les règles de calcul pour contrôler les largeurs des fissurations sont dérivées. Et de plus, l'application pratique du système du béton armé précontraint et l'application duquel au pont de Kamihimekawa, qui est le pont en cadre en forme de π , sont décrites dans ce rapport.

ZUSAMMENFASSUNG

Das Riss-und Verformungsverhalten des Spannstahlbetons wird sowohl unter der statischen Belastung wie unter der dynamischen Belastung untersucht. In Bezug auf das Rissverhalten werden der anfängliche sowie der stationäre Zustand betrachtet. Die Konstruktionsregeln zur Rissekontrolle werden aufgestellt. Auch stellt dieser Beitrag die Praxis des Spannstahlbeton-Systems und dessen Anwendung auf eine π -förmige Rahmenbrücke über dem Fluss Kamihime dar.